Green Chemistry

Accepted Manuscript

ROYAL SOCIETY OF CHEMISTRY

www.rsc.org/greenchem

Green Chemistry

ARTICLE

Precise Oxygen Scission of Lignin Derived Aryl Ethers to Quantitatively Produce Aromatic Hydrocarbons in Water

Received 00th xx 20xx,
Accepted 00th xx 20xx

DOI: 10.1039/x0xx00000x

www.rsc.org/

Zhicheng Luo,[a] YimengWang,[a] Mingyuan He,[a] Chen Zhao*[a]

To produce aromatic hydrocarbons from biomass, a novel route is reported for one-pot selective hydrodeoxygenation of lignin derived aryl ether mixture to C_6-C_9 aromatic hydrocarbons over Ru/sulfate zirconia in aqueous phase. The cascade steps undergo the initial precise cleavage of $C_{aliphatic}$-O bond of phenolic dimers or $C_{aromatic}$-OCH_3 of phenolic monomers, as well as the full blockage of benzene-ring and cyclic-alkene hydrogenation to realize nearly quantitative aromatic hydrocarbons formation at 240 °C in presence of a low pressurized H_2 (2 - 8 bar). With Ru catalyst, the primary step in competition of hydrogenolysis of C-O bond as well as hydrogenation of benzene ring is shown to be sensitive to temperatures and hydrogen pressures, which can subtly modify the concentrations and spatial distributions of the surface adsorbed H·. A high temperature and a low hydrogen pressure are found to be essential for hydrogenolysis, since the H· species nearby the oxygen atom are more strongly adsorbed at such conditions and thus preferred to be reserved on the Ru surface. Herein it is defined as "atom-induced H sorption effect", probably resulted from the analogous hydrogen-bond force between adsorbed H· with the adjacent oxygen atom on the metal surface. Besides the initial step, another key point for aromatic hydrocarbons formation is to optimize the target route of cycloalkene dehydrogenation, but suppressing the parallel hydrogenation pathway to saturated cycloalkane. It is found that the produced phenol intermediate serves as the proper H-acceptor at selected catalytic system during the whole conversion, via fast consuming the in-situ produced H· from cyclohexene dehydrogenation. Such interesting phenomenon of internal hydrogen transfer not only promotes the dehydrogenation and hydrogenation equilibrium on cyclohexene but also lowers the in-situ H· concentration on the Ru surface, both of which would be beneficial for reaching a high benzene yield. This hypothesis for internal hydrogen transfer is further confirmed by separate experiments and density functional theory modelling results.

Introduction

The efficient utilization of lignocellulose biomass has attracted increasing attention.[1] As the second abundant lignocellulosic resource, lignin is a three-dimensional highly branched aromatic bio-polymer composed of various C-O linkages connected with methoxylated phenyl-propane units. Through depolymerization, lignin is converted to diverse aryl ether fragments comprising of $C_{aromatic}$-OCH_3, $C_{aromatic}$-O-$C_{aromatic}$, and $C_{aromatic}$- O-$C_{aliphatic}$ units.[2] These phenolic fragments are rich in inherent aromatic structures with high energy-density, but the technique for precise removal of oxygen in these bio-derived molecules to produce aromatic hydrocarbons has been a challenging issue.[3]

Because of the high C-O bond dissociation energy of aryl ethers (218-314 kJ·mol^{-1})[4], it is contradictory to break down the ether bonds in presence of H_2 without hydrogenation of benzene-ring. Parallel hydrotreating routes including partial/ full hydrogenation of benzene-ring, hydrogenolysis of $C_{aromatic}$-O bonds, and hydrogenolysis of $C_{aliphatic}$-O bonds co-exist, and therefore, it is quite arduous to select a specific selective route to defunctionalize the oxygen-containing groups as well as simultaneously protect the benzene-rings in liquid phase.

Previous researches are primarily aimed at cleaving of the C-O bonds of lignin derived fragments in the liquid phase. The homogeneous catalysts[5] such as Ni[5a], Ru[5b], V[5c] complexes, as well as unsupported nanoparticles Fe[6] and RuNi[7a], AuNi[7b], are capable in selective hydrogenolysis of lignin-derived aryl ethers to a mixture of aromatics and phenolics/cycloalcohols in solvents under mild conditions. Besides, the heterogeneous Ni-based catalysts shows considerable activities in cleaving the $C_{aliphatic}$–O bond of aryl ethers to produce aromatics and cycloalcohols in the liquid phase, as well.[8] The various –OCH_3 substituted phenolic ethers can also be quantitatively hydrodeoxygenated to cyclic alkanes with the bifunctional metal/acid catalysts in water.[9] Phenols can be dehydroxylated by combined Raney Ni and HBEA catalysts using 2-PrOH as H-donor.[10] In the non-polar solvent decane, bimetallic FeMoP catalyst can selectively cleave C–O bonds of aryl ethers to produce aromatics at a high temperature of 400 °C.[11] Apart

[a] Shanghai Key Laboratory of Green Chemistry and Chemical Processes, School of Chemistry and Molecular Engineering, East China Normal University, Shanghai 200062, China. E-mail: czhao@chem.ecnu.edu.cn

Electronic Supplementary Information (ESI) available: [details of any supplementary information available should be included here]. See DOI: 10.1039/x0xx00000x

ARTICLE

from the reactions occurred in the liquid phase, MoO_3 was shown to be active for hydrodeoxygenation of phenolic monomers to high yields of aromatic hydrocarbons in the gas phase.[12]

Water is present ubiquitously in the biomass resource, and is a green and excellent solvent for upgrading of biomass derived oxygenates as well. However, in neat aqueous phase it has not been reported that lignin derived aryl ethers can be selectively converted to more valuable aromatic hydrocarbons in a one-step process. Herein, in this contribution we report a new approach to selectively cleave and deoxygenate the aryl ether mixture to C_6-C_9 aromatic hydrocarbons with a multi-functional Ru/sulfate zirconia (SZ) catalyst in aqueous phase *via* cascade steps.

Results and discussion

Selective cleavage and hydrodeoxygenation of phenethoxy-benzene (β-O-4 model compound of lignin) in water.

Lignin depolymerization generates an abundant variety of phenolic aryl ethers.[3] Firstly, a representative β-O-4 model compound (contributing to 45-62% C-O linkages in lignin), phenethoxybenzene (PEB, ^{1}H and ^{13}C NMR spectra were displayed in Fig. S1) is selected to investigate the proper route for aromatics formation. In the blank test, PEB was inactive in the high-temperature water. In the whole hydrodeoxygenation process, metal centers may greatly influence the pathways and rates of individual steps. To explore the effect of three metals in water, Ru/C, Pt/C, and Pd/C (5 wt%) were comparatively studied at 240 °C in presence of 8 bar H_2 in aqueous phase (see Fig. S2). The results (Table S1) showed that Ru/C and Pd/C both catalyzed high hydrogenolysis rates on PEB (165 and 270 *m*mol·g^{-1}·h^{-1}, respectively), while Pt/C performed poorly with a slow rate of 47 *m*mol·g^{-1}·h^{-1}. The parallel route of hydrogenation of benzene ring was shown to be active on Pd/C site (rate: 47 *m*mol·g^{-1}·h^{-1}), whereas it was almost inert with Ru/C (3.3 *m*mol·g^{-1}·h^{-1}). Through the rate comparison of hydrogenolysis to hydrogenation, Ru/C is more capable than Pd/C for selective hydrogenolysis (hydrogenolysis / hydrogenation ratio = 55) of the C-O bond of PEB (see Table S1).

It should be addressed that the Ru based catalysts, e.g. Ru/C, have already exhibited uniquely high selectivity in hydrogenolysis of C-O bonds in polyols [13] and cellulose. [14] For achieving a more selective route for hydrogenolysis of C-O bond, Ru/C is thus selected for further investigation. Kinetics of PEB conversion with Ru/C at identical conditions (see Fig. 1a) revealed that at an initial time PEB was cleaved to C_6 phenol and C_8 ethyl-benzene with nearly 100% selectivity. It is notable that it does not produce any benzene-ring hydrogenation products, as well as the cleaved products of C_6 benzene and C_8 phenyl ethanol (see Fig. 1a). This indicates that at optimized conditions, Ru catalyzes the exclusive route for cleaving of the $C_{aliphatic}$-O bond of PEB, while fully blocking the possible hydrogenation pathway on benzene-ring and the hydrogenolysis route on $C_{aromatic}$-O bond (Scheme S1). As a function of time, the intermediate phenol was converted to cyclohexanone and cyclohexanol with a rapid rate over Ru/C, and by contrast, the other intermediate ethyl-benzene was quite stable without any reacting. Such great hydrogenation rate disparity was further evidenced by the separate experiment that *co*-introduction of phenol and ethyl-benzene over Ru/C led to a high phenol hydrogenation rate of 96 *m*mol·g^{-1}·h^{-1}, and by contrast a slow rate for ethyl-benzene hydrogenation (7.0 *m*mol·g^{-1}·h^{-1}) at identical conditions (Fig. S3), probably attributed to the better solubility of phenol in water as well as the stronger adsorption of phenolic –OH groups than ethyl-benzene on the Ru site, as similar as the case on the Ni surface.[8b] In addition, it can be also observed that a small part of benzene (5% yield) was formed from PEB over Ru/C in high-temperature water at 100 min.

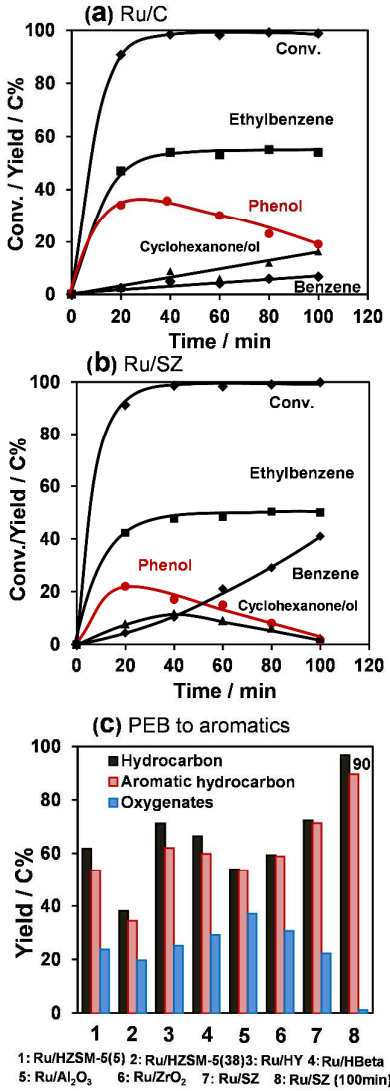

Figure 1. (a) Ru/C (0.10 g) and (b) Ru/SZ (0.10 g) catalyzed PEB hydrodeoxygenation as a function of time. (c) Selective hydrogenation of PEB to aromatic hydrocarbons over diverse supported Ru catalysts (5 wt.%, 0.10 g) for 1 h. General conditions: PEB (1.0 g), H_2O (100 mL), 240 °C, 8 bar H_2, stirring at 650 rpm.

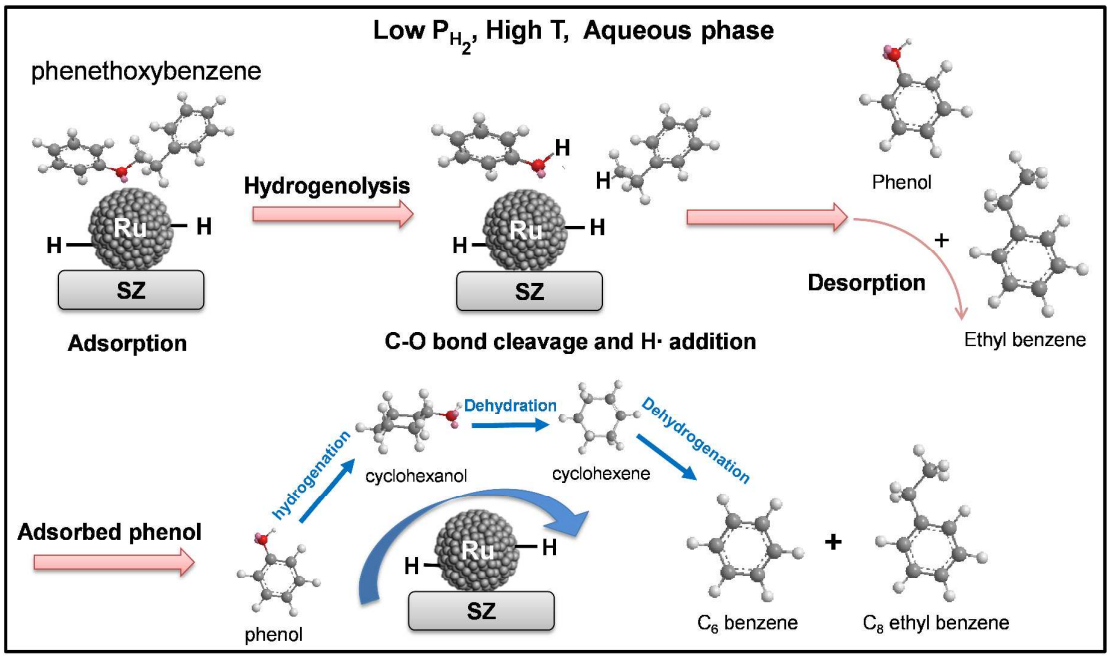

Scheme 1. The designed reaction pathway for Ru/SZ catalyzed selective hydrodeoxygenation of PEB to aromatic hydrocarbons in aqueous phase.

The further strategy for target C_6 aromatic hydrocarbon formation is designed as dehydration of as-received cyclohexanol over acid sites, subsequently dehydrogenation of the formed cyclohexene to benzene with metal sites at a low hydrogen pressure, *via* suppressing the by-product cyclohexane formation (*see* Scheme 1). To achieve it, some Ru catalysts supported on solid acids were tested for catalyzing the cascade reactions (*see* Figs. 1b and 1c). With Lewis acids supported Ru such as Ru/Al_2O_3 and Ru/ZrO_2, the cyclohexanol intermediate was stable at 35-40%, implying that Lewis acid sites are not active for dehydration in the selected aqueous system.[9b] Compared to H-zeolites supported Ru/HY (5), Ru/HBeta (20), Ru/HZSM-5 (5), and Ru/HZSM-5 (38), the Ru/sulfate zirconia (SZ) sample catalyzed a much higher yield (73%) of C_6 benzene and C_8 ethyl-benzene for 1 h. If extending the reaction time to 100 min., 90% C_6 and C_8 aromatic hydrocarbons can be achieved on Ru/SZ. Based on these results, it is implied that the addition of SZ may facilitate cyclohexanol dehydration to cyclohexene, and the produced cyclohexene is selectively dehydrogenated to the target benzene at the selected condition with a high temperature and a low H_2 pressure (240 °C, 8 bar H_2). The kinetics of PEB conversion to aromatics over Ru/SZ (Fig. 1b) revealed that Ru/SZ is capable of catalyzing all cascade steps including C-O bond cleavage of PEB (188 $m$mol·g^{-1}·h^{-1}), phenol hydrogenation to cyclohexanol, cyclohexanol dehydration to cyclohexene, as well as cyclohexene dehydrogenation to benzene, and therefore, it leads to the highly selective aromatics formation *via* the integrated steps.

The characterization of Ru/SZ feathered that Ru nanoparticles (synthesized by liquid phase HCHO reduction) were shown to be uniform at sizes of 2.0 ± 0.4 nm, as demonstrated by TEM image (supporting information at Fig. S4a). The high-resolution TEM image illuminated that Ru nanoparticles are of high crystallinity, composed by multi-crystalline particles with exposed major Ru (100) facets, as well as some minor Ru (111) and Ru (110) facets (Fig. S4b). Determined from the CO chemisorption measurement, the Ru dispersion was 21%. SEM images (Fig. S4c) illuminated that the Ru/SZ sample exhibited granulated and inhomogeneous shape with a crystal size of around 1-10 μm. The acid site was determined to be 0.1078 $m$mol·g^{-1}, as characterized by the temperature programmed desorption of ammonia (Fig. S4d). These results indicate that Ru nanoparticles are well dispersed on the acidic SZ carrier, constructing to a bi- or multi-functional catalyst.

Controlling the primary step of hydrogenolysis and hydrogenation of PEB over Ru/SZ in water.

The crucial competing routes of hydrogenolysis (at position a or b) and hydrogenation (partial and full) can be substantially influenced *via* the adsorbed H· on the Ru/SZ surface (scheme S1). The surface adsorbed H· is determined by multi-factors. The influence of H_2 pressure (see Fig. 2a) demonstrated that hydrogenolysis played as the major role in presence of a relatively low H_2 pressure (≤ 10 bar) at 240 °C, and PEB was selectively cleaved at the $C_{aliphatic}$-O position to produce C_6 phenol and C_8 ethyl-benzene. When the H_2 pressure was increased to 30 bar, the major reaction pathway was altered to full hydrogenation (Fig. S5a). It indicates that the relatively high concentrations of activated H· (at high H_2 pressure) mainly contribute to the hydrogenation of PEB, and as well accelerate the cleavage rate of $C_{aromatic}$-O of PEB. Consequently,

ARTICLE

the high H_2 pressure leads to a complicated and unselective product distribution, and the desired aromatic hydrocarbons such as ethyl-benzene and benzene were substantially hydrogenated to cycloalkanes. In explaining the effect of hydrogen pressures, it is assumed that at the low H_2 pressures such as 2 bar, the surface adsorption sites are probably not fully occupied, and with the increasing H· incorporation by introducing a higher-pressure H_2, the H· concentrations around the benzene-rings will be greatly accumulated to accelerate the hydrogenation rates since that PEB is preferably adsorbed in the planar mode with an adsorption energy of 262 kJ·mol^{-1}, as determined from the DFT modelling result (Fig. S6).

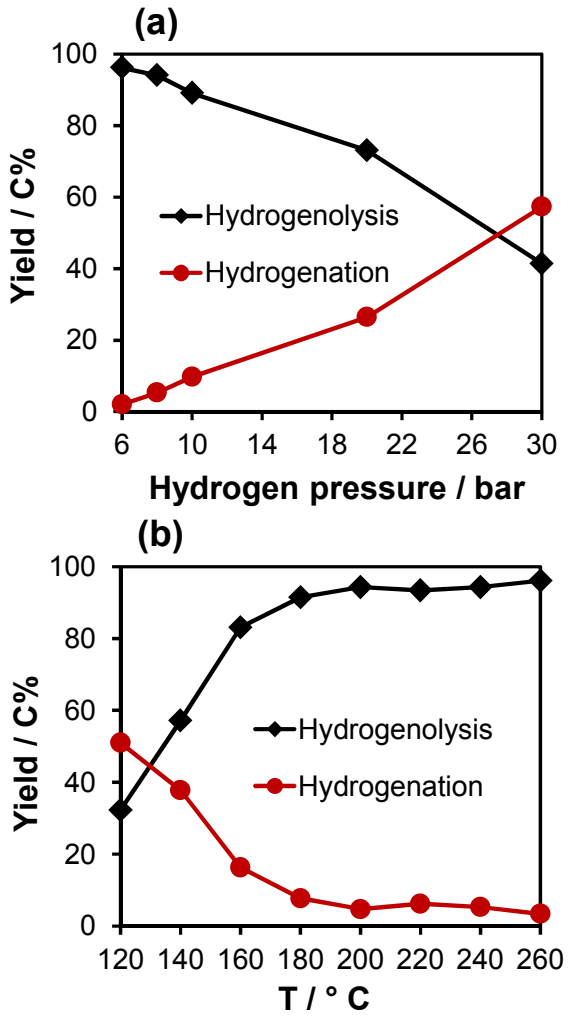

Figure 2. Influence of (a) hydrogen pressure and (b) temperature towards hydrogenolysis and hydrogenation of PEB over Ru/SZ. Reaction conditions: PEB (1.0 g), Ru/SZ (5 wt.%, 0.10 g), H_2O (100 mL), 1 h, stirring at 650 rpm, (a) 240 °C, (b) 8 bar H_2.

In addition to the hydrogen pressure, the temperature effect manifested that at relative low temperatures (120 - 200 °C, 8 bar H_2), hydrogenation as well as hydrogenolysis (at positions a and b, Scheme S1) co-existed (see Fig. 2b). With the increasing temperatures from 200 to 260 °C, hydrogenolysis dominated as the major route (yield > 95%), and hydrogenation occurred in a minor part (see Fig. S5b), suggesting that a high temperature, e.g., 240 °C, benefits for the cleavage of $C_{aliphatic}$-O bond of PEB (95% selectivity). Due to the much lower C-O bond dissociation energy barrier, [4] the $C_{aliphatic}$-O bond rather than $C_{aromatic}$-O bond of PEB is cleaved at a higher temperature.

The change of temperatures may modify the status of the surface adsorbed H· species. Concerning on the concentrations of surface adsorbed H· species, it is commonly recognized that such H· species will be preferably desorbed at increasingly high temperatures, especially when the adsorption of H· on the metal surface is exothermic with a typical enthalpy value of -125 to -150 kJ·mol^{-1}.[15] Additionally, the higher temperature would lower the solubility of hydrogen gas in the selected aqueous system.[16] In order to track the concentration of adsorbed H· on the surface of Ru/SZ at two different reaction temperatures (120 °C and 240 °C) in presence of 8 bar H_2, temperature programmed desorption of H· (from 80 °C to 350 °C) was performed on the used Ru/SZ (after reaction with PEB at designated conditions) in a He flow monitored by a mass spectrometry. In the blank test with the fresh catalyst Ru/SZ, no signal was obtained either with thermal conductivity detector or with mass spectroscopy detector (Fig. 3a). The physisorbed H· was then removed by heating at 80 °C in a He flow for 0.5 h, and only the chemisorbed H· was reserved. With the increasing temperatures, the two-state peaks appeared at 150 °C and 300 °C detected by temperature programmed desorption may be correlated with the occupation of threefold Ru sites on the hcp and fcc facets, respectively, as suggested by Feulner and Menzel[17]. The results manifested that the surface adsorbed H· was more abundant at the reaction temperature of 120 °C than that at 240 °C, as compared by the normalized areas of the detected H· signals (Fig. 3a).

Besides the evidence derived from the detected surface H· species at two working temperatures tracked by temperature programmed desorption, we design another experiment, that is, phenol hydrogenation over Ru/SZ in presence of 8 bar H_2 with varying temperatures (Fig. 3b). The results showed that the rate for phenol hydrogenation sharply decreased from 285 to 66 *m*mol·g^{-1}·h^{-1} when the temperature was increased from 160 to 260 °C. The rate express for phenol hydrogenation is $r = k\cdot[\text{phenol}_{ads}]^a\cdot[H_{ads}]^b$. In principle, the solubility of phenol in water is infinite above 65 °C, and the reaction orders of phenol (a) and hydrogen (b) are positive.[18] This implies that the increase of temperature would not change the concentration of adsorbed phenol, and the rate constant *k* should be increased. However, oppositely the obtained overall rate was decreased. Based on the rate equation, it is rationally inferred that the reduced surface adsorbed H· species $[H_{ads}]$ at higher temperatures leads to the lower hydrogenation rate on phenol, when the value ($k\times[\text{phenol}_{ads}]^a$) is increased.

With these two reliable proofs, it can be firmly concluded that the higher temperatures (at selected range) would lower

the concentrations of surface adsorbed H·. However, this gained information cannot fully explain the changed ratios of hydrogenolysis to hydrogenation with temperature variations as displayed at Fig. 2b, as the aromatic benzene rings of PEB are adsorbed in a planar model, which suggests that in principle the hydrogenation of benzene ring is more favored even with few adsorbed H· species on the Ru surface. We may argue that hydrogenation of benzene ring needs higher amounts of metal-activated H· than hydrogenolysis of C-O bonds, but this argument also cannot intrinsically support the observed experimental phenomenon when the aromatic rings are planarly-adsorbed.

The only probable reason is that the higher temperatures change the surface adsorbed H· species not only by the concentrations, but also by the spacial distributions. In another word, the weaker adsorbed H· species on the Ru surface surrounding the benzene rings will be fast desorbed as the temperature increases, while the H· species nearby the oxygen atoms are strongly adsorbed due to the induction by the oxygen atom of PEB, and thus are reserved on the Ru surface even with a rising temperature (Fig. 3c). We define such phenomenon as “atom-induced H adsorption effect”.

In fact, the electron of 1s (H) prefers to shift to the empty orbital of 4d (Ru) when H· is adsorbed on the Ru surface,[15] and this leads to form a strong analogous hydrogen-bond force between the electron-deficient orbital of 1s (H) and electron-rich orbital of 2p (O) (Fig. 3d). Such force induces a strong H· adsorption strength on the Ru surface. In comparison, π or P-π conjugation makes the benzene rings highly stable, and thus, weakens the available interaction of adsorbed H· with benzene rings of PEB (Fig. 3d). Resultantly a high selectivity of hydrogenolysis of the C-O bond rather than hydrogenation of benzene-rings is attained with few adsorbed H· species.

Therefore, the competition of hydrogenolysis to hydrogenation depends on the concentration together with the strength of adsorbed H· at working conditions. If the adsorbed H· is abundant, the rates of hydrogenation and hydrogenolysis are both speeded up. When the H· concentration is decreased, a great disparity on strength of adsorbed H· nearby the oxygen atom and benzene rings of PEB leads to the high selectivity to the hydrogenolysis route on C-O bond. With the variation of temperatures and H_2 pressures, the reaction pathways for PEB conversion over Ru/SZ are depicted at Scheme S2. The low temperatures and high H_2 pressures are beneficial for the partial and full hydrogenation, together with the hydrogenolysis route on $C_{aromatic}$-O bond at position *a*. However, the targeted ether cleavage route in the whole designed hydrodeoxygenation process favors the specific conditions of the relatively high temperature and low H_2 pressure.

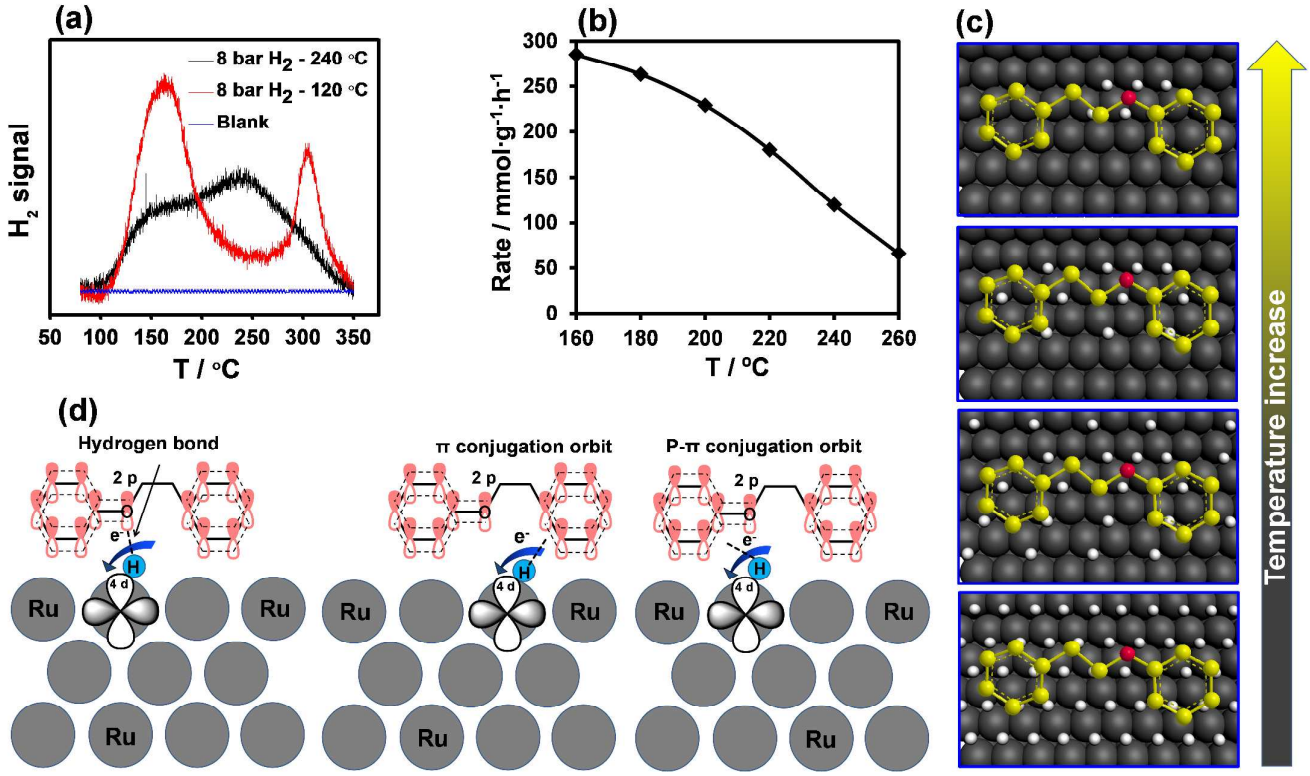

Figure 3. (a) Temperature programmed desorption of adsorbed H· on the used Ru/SZ (after adsorption of 8 bar H_2 in water at 120 °C or 240 °C for 1 h, (b) Rates of hydrodeoxygenation of phenol over Ru/SZ by different temperatures, reaction conditions: Phenol (1.0 g), Ru/SZ (5 wt.%, 0.10 g), H_2O (100 mL), 8 bar H_2, 1 h, stirring at 650 rpm. (c) Hydrogen adsorption over the Ru surface at different temperatures, white atom: H, red atom: oxygen, yellow atom: carbon. (d) Different interactions between activated H· species with oxygen atom and double benzene rings of PEB on the Ru surface.

ARTICLE

Controlling the critical step of cyclohexene dehydrogenation over Ru/SZ in water.

In the overall PEB hydrodeoxygenation process to aromatic hydrocarbons, the critical step is controlling the selectivity of the individual step of cyclohexene dehydrogenation to benzene, and meanwhile preventing the parallel step of cyclohexene hydrogenation to cyclohexane. Calculated by HSC software, the thermodynamic data for cyclohexene conversion to benzene and cyclohexane at 240 °C are displayed at Figure 4. It shows that in the dehydrogenation reaction for forming benzene, ΔG equals to -10.4 kJ·mol^{-1} within an endothermic reaction (ΔH = 26.9 kJ·mol^{-1}), while the other direction for forming cyclohexane is exothermic (ΔH = - 24.7 kJ·mol^{-1}) and ΔG equals to -6.9 kJ·mol^{-1}. By comparing the thermodynamic data, it is suggested that dehydrogenation of cyclohexene to benzene is more preferred at 240 °C under the ideal conditions when the reaction approaches to the thermodynamic equilibrium.

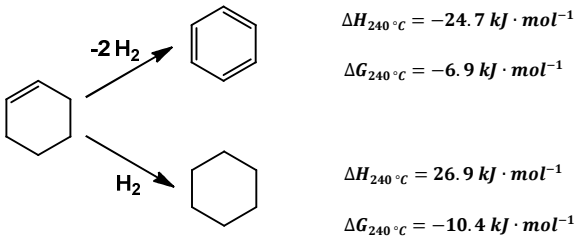

Figure 4. Thermodynamic data for dehydrogenation/hydrogenation of cyclohexene to benzene or cyclohexane.

To explore the key step of cyclohexene dehydrogenation, this individual step was separately investigated over Ru/SZ at selected condition (240 °C, 8 bar H_2, see Fig. 5). Unexpectedly, cyclohexane but not benzene was the solo product from cyclohexene conversion with 100% selectively with Ru/SZ in the aqueous phase. Considering that in the overall PEB conversion over Ru/SZ, phenol and cyclohexanol were the two major intermediates during the conversion (see Fig. 1b), the *co*-reactions of cyclohexene and cyclohexanol/phenol were conducted afterwards. These results showed that *co*-reacted with cyclohexanol and cyclohexene, the selectivity to benzene was increased to 40%, and more surprisingly, the target benzene was enhanced to 90% when *co*-reacting of phenol and cyclohexene at 240 °C in presence of 8 bar H_2. The high selectivity of benzene is speculated to the reason that the phenol intermediate serves as the H-acceptor, which can digest the in-situ produced H_2 from cyclohexene dehydrogenation. The consumption of H_2 not only promotes the dehydrogenation and hydrogenation equilibrium on cyclohexene but also lowers the in-situ H· concentration on the Ru surface, both of which would be beneficial for reaching a high benzene yield. This is further proven by the comparative experiment that in presence of N_2, *co*-reaction of cyclohexene and phenol led to the formation of 100% selectivity of benzene from cyclohexene dehydrogenation, and phenol was partially converted to cyclohexanol. The internal H-transfer between cyclohexene dehydrogenation and phenol hydrogenation at selected condition helps shifting the reaction route to specifically produce the dehydrogenated product benzene.

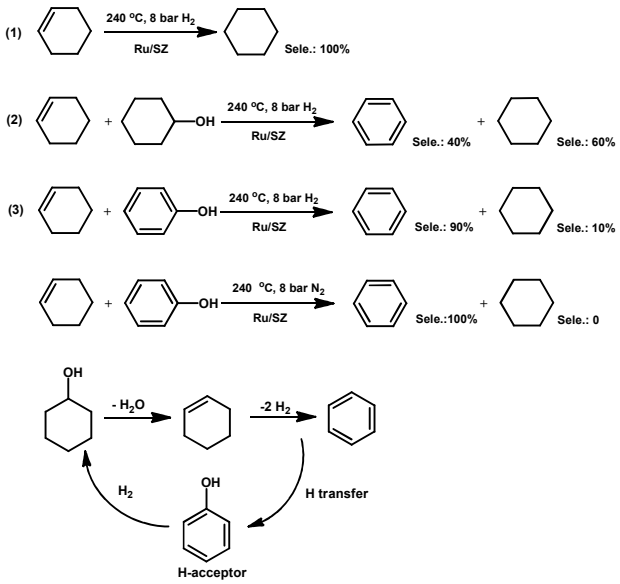

Figure 5. The reaction of cyclohexene (1), and co-reaction of cyclohexene and cyclohexanol (2), co-reaction of cyclohexene and phenol (3) over Ru/SZ in presence or absence of H_2 in the aqueous phase. Reaction conditions: cyclohexene (1.0 g) or mixture of cyclohexanol (0.5 g) and cyclohexene (0.5 g) or mixture of phenol (0.5 g) and cyclohexene (0.5 g), H_2O (100 mL), 240 °C, 8 bar H_2 or N_2, 1 h.

In the theory of internal hydrogen transfer between cyclohexene dehydrogenation and phenol hydrogenation, it is assumed that phenol is more preferably adsorbed on the Ru surface than cyclohexene. Under such condition, then the adsorbed phenol can easily accept the *in-situ* generated H· from cyclohexene dehydrogenation to complete the internal hydrogen transfer process. To verify this assumption, the adsorption energies of five intermediates (ethyl-benzene, phenol, cyclohexanol, cyclohexanone, and cyclohexene) from PEB conversion were calculated by DFT on Ru (0001) surface (see Table 1). The DFT modelling results demonstrated that on the clean Ru (0001) surface, the adsorption energies followed the order, E_{ads} (phenol) > E_{ads} (ethyl-benzene) > E_{ads} (cyclohexanone) > E_{ads} (cyclohexanol) > E_{ads} (cyclohexene). If calculated on the Ru (0001) surface with a water mono-layer, the adsorption energies of these compounds were decreased due to the introduced water interference, but the order trend was not changed, that is, the adsorption energy of phenol (-160 kJ·mol^{-1}) was still the highest among these compounds, and was four times higher than that of cyclohexene (-26 kJ·mol^{-1}). These DFT results confirm our inference that the adsorption of phenol is much stronger than other intermediates, and therefore, the presence of phenol as H-acceptor is the critical factor for manipulating the individual step of cyclohexene dehydrogenation.

Table 1. Adsorption energies of reaction intermediates on Ru (0001) surface calculated by DFT.

	Clean surface ($kJ \cdot mol^{-1}$)	With water monolayer ($kJ \cdot mol^{-1}$)
Ethyl-benzene	-148	-118
Phenol	-172	-160
Cyclohexanol	-49	-32
Cyclohexanone	-77	-68
Cyclohexene	-76	-26

Selective hydrodeoxygenation of lignin-derived diverse aryl ethers to aromatic hydrocarbons in water.

Based on the obtained knowledge, the designed catalytic system was applied to hydrodeoxygenate the lignin derived representative phenolic dimmers including β-O-4, α-O-4, and 4-O-5 model compounds (see Fig.6). These aryl ether compounds were selectively hydrodeoxygenated to C_6, C_7, and C_8 aromatic hydrocarbons with yields exceeding 78% over Ru/SZ in water at 240 °C with 8 bar H_2 for 1.5 h.

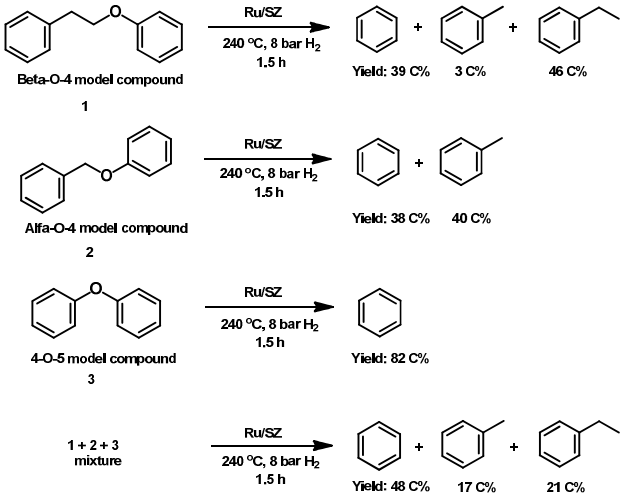

Figure 6. Selective hydrodeoxygenation of lignin derived phenolic dimers or mixture to aromatic hydrocarbons over Ru/SZ in water. Reaction condition: each reactant (5 *m*mol), Ru/SZ (5 wt.%, 0.10 g), H_2O (100 mL), 240 °C, 8 bar H_2, stirring at 650 rpm. In the conversion of a phenolic dimer mixture, each compound (2.5 *m*mol) and Ru/SZ (5 wt.%, 0.15 g) were used.

The oxygen elimination route follows the similar mechanism as PEB conversion (see Scheme 1), that is, the initial selective cleavage of ether bond to produce phenol and aromatics, followed by a dedicatedly designed route for sequential hydrogenation of phenol, dehydration of cyclohexanol, and dehydrogenation of cyclohexene to benzene. It should be noted that the side reactions of hydrogenation of ether reactants and aromatic hydrocarbons are well suppressed. Even treating with a mixture of β-O-4, α-O-4, and 4-O-5 aryl ethers with an equal molar ratio, a high yield (86%) of C_6-C_8 aromatics mixture was obtained from the one-pot hydrodeoxygenation process with Ru/SZ at the optimized condition of 240 °C in presence of 8 bar H_2 for 1.5 h (see Fig.6 and Fig. S7).

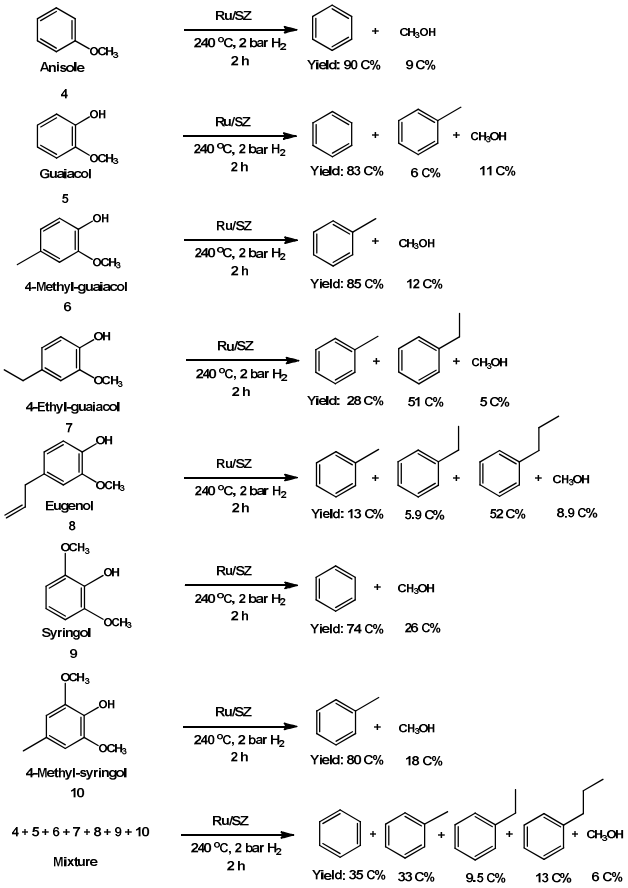

Figure 7. Selective hydrodeoxygenation of lignin derived phenolic monomers or mixture to aromatic hydrocarbons over Ru/SZ in water. Reaction condition: reactant (1.5 *m*mol), Ru/SZ (5 wt%, 0.20 g), H_2O (100 mL), 240 °C, 2 bar H_2 and 6 bar N_2, 2 h, stirring at 650 rpm.

Apart from the phenolic dimers, there are substantial amounts of substituted phenolic monomers formed from lignin degradation. They have two types of oxygen-containing groups, that is, the phenolic –OH and $–OCH_3$ groups. Through lowering the hydrogen pressure to 2 bar (with additional 6 bar N_2), the conversion of anisole and guaiacol reached nearly 90% yields of C_6 benzene at 240 °C after selectively removing the phenolic –OH and/or $–OCH_3$ groups over Ru/SZ in aqueous phase (see Fig.7). In the conversion of guaiacol, in addition to 83% yield of benzene, 6% yield of toluene was also formed due to the recombination of CH_3OH with the benzene ring. When 4-methyl-, 4-ethyl-, and 4-*n*-allyl- substituted guaiacols were hydrodeoxygenated, the yields of aromatic hydrocarbons were lowered to respective 85%, 79%, and 71% (see Fig.7), indicating the rates for hydrogenation of aryl-benzenes to saturated cycloalkanes were highly accelerated on Ru/SZ. This was verified by the experimental data that the hydrogenation yield on toluene (35%) was 7% lower than that on ethyl-benzene (42%) at same reaction conditions (Table S2). In addition, the C-C alkylation products with substituted phenol

and methanol were not observed. It was tested that alkylation of 4-methyl-, 4-ethyl-, and 4-*n*-propyl- substituted phenol with methanol did not occur at selected conditions in aqueous phase (Table S3), suggesting that two-molecular C-C coupling reactions are difficult to be catalyzed with solid acids in aqueous phase albeit that these solid acids are effective in the gas phase or solvent-less environment. The more complex substituted syringols were also quantitatively converted to aromatic hydrocarbons at selected condition. In principle, the mechanisms for cleaving the $C_{aromatic}$-OH and $C_{aromatic}$-OCH_3 of phenolic monomers are different from that of phenolic dimers. The presence of large amounts of aryl phenols and methanol implies that the hydrogenolysis of the $C_{aromatic}$-OCH_3 bond but not the CH_3-O bond appears as the primary step for conversion of –OCH_3 substituted phenols.

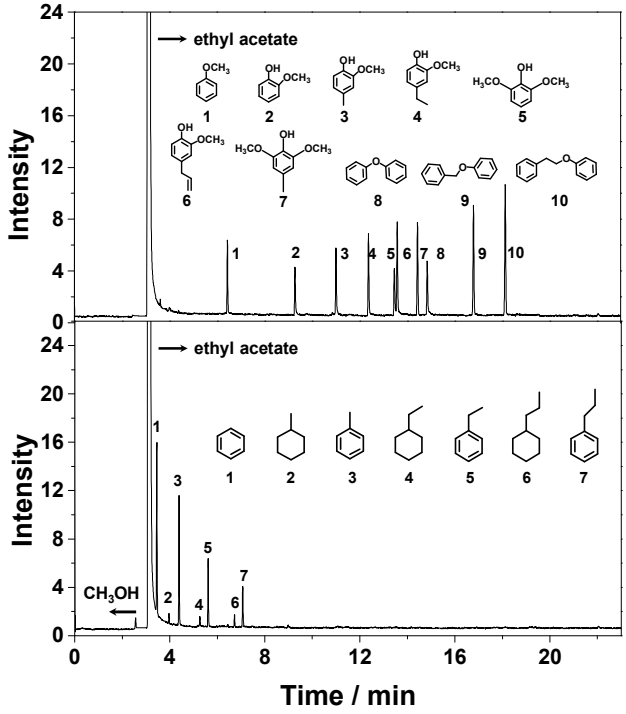

Figure 8. GC chromatography spectra of (a) a reactant mixture of phenolic monomers and dimers, and (b) aromatic hydrocarbon products after one-pot selective hydrodeoxygenation of (a) mixed aryl ethers over Ru/SZ in aqueous phase. Reaction conditions: each compound (0.3125 *m*mol), Ru/SZ (5 wt%, 0.5 g), H_2O (100 mL), 240 °C, 2 bar H_2 and 6 bar N_2, 5 h, stirring at 650 rpm. After reaction, ethyl acetate was used as solvent to extract the organic products.

Selective hydrodeoxygenation of an aqueous mixture of seven kinds of phenolic monomer mixture (anisole, guaiacols, and syringols) allowed to quantitatively convert it to aromatic hydrocarbons mixtures including C_6 benzene (35% yield), C_7 toluene (33% yield), C_8 ethyl-benzene (9.5% yield), and C_9 propyl-benzene (13% yield) at 240 °C in presence of a low hydrogen pressure of 2 bar (see Fig. 7 and Fig. S8a). In the aqueous phase, methanol was produced from the hydrogenolysis of $C_{aromatic}$–OCH_3 group of phenolic ethers. The carbon balance exceeded 95% in the liquid phase. In the gas phase, only a trace amount of CH_4 was detected (see Fig. S8b). Furthermore, almost quantitative transformation of mixed ten kinds of phenolic dimer and monomer ethers to aromatics (95% yield, consisting of 40% C_6, 29% C_7, 16% C_8, and 9.4% C_9 hydrocarbons) in a one-step process (see Fig. 8) verifies that such developed system exerts the selective hydrodeoxygenation capability for aromatics formation from a variety of phenolic aryl ethers. It should be addressed that such C_6-C_9 aromatic hydrocarbon products mirrored the distribution of ether reactants in the mixed phenolic oil (see Fig. 5), suggesting that no polymerization occurs during the integrated process and a high feasibility to further deoxygenate of lignin derived complex oil ingredients. The novel and cascade hydrodeoxygenation reaction steps towards aryl ethers leads to a highly integrated atom-economic process for aromatic hydrocarbons formation *via* a subtly-manipulated reaction route.

Conclusions

A novel route is established for one-pot hydrodeoxygenation of lignin derived aryl ether mixture to C_6-C_9 aromatic hydrocarbons over Ru/SZ in the aqueous phase. The multi-functional Ru/SZ catalyzes the selective cleavage of $C_{aliphatic}$-O bond of phenolic dimers or $C_{aromatic}$-OCH_3 of phenolic monomers, as well as the full blockage of benzene-rings hydrogenation, finally reaching the cascade steps to realize nearly quantitative aromatic hydrocarbons formation at 240 °C in presence of a low pressure H_2. In manipulating the selectivity to aromatic hydrocarbons with Ru catalysts, the primary step is to operate the competition step of hydrogenolysis and hydrogenation, which depends on the concentration together with the strength of adsorbed H· at working conditions. When the H· concentration is decreased at high temperatures or low H_2 pressures, a great disparity on strength of adsorbed H· species that are nearby the benzene rings and oxygen atoms (atom-induced H adsorption effect) leads to the high selectivity to the hydrogenolysis route on the C-O bond of aryl ethers.

In addition, the controlling of the individual target step of cyclohexene dehydrogenation is successfully realized by an internal hydrogen transfer between cyclohexene dehydrogenation and phenol hydrogenation in aqueous phase over Ru/SZ at selected conditions. The function of phenol (acting as H· acceptor) not only promotes the dehydrogenation and hydrogenation equilibrium on cyclohexene but also lowers the in-situ H· concentration on the Ru surface, both of which would be positive for reaching a high yield of aromatic hydrocarbons. Proper metal site (Ru) and solid acid (SZ), together with a favourable low hydrogen pressure (2-8 bar) and a relative high temperature (240 °C) are crucial factors for precisely coordinating multi-steps to achieve target routes and aromatic hydrocarbons. This established selective route provides a new promising technique for directly producing a green aromatics pool from lignin derived bio-oil.

Acknowledgements

This research was supported by the Recruitment Program of Global Young Experts (Thousand Youth Talents Plan), National Natural Science Foundation of China (Grant No: 21573075), and Shanghai Pujiang ProgramPJ1403500.

Notes and references

1. (a) G. W. Huber, S. Iborra and A. Corma, *Chem. Rev*. 2006, **106**, 4044-4098; (b) J. S. Luterbacher, J. M. Rand, D. M. Alonso, J. Han, J. T. Youngquist, C. T. Maravelias, B. F. Pleger and J. A. Dumesic, *Science,* 2014**, 343**, 277-280; (c) J. N. Chheda, G. W. Huber and J. A. Dumesic, *Angew. Chem. Int. Ed*, 2007, **46**, 7164-7183; (d) T. R. Carlson, Y.T. Cheng, J. Jae and G. W. Huber, *Energy Environ. Sci*., 2011, **4**, 145-161.
2. (a) Q. Song, F. Wang and J. Xu, *Chem. Commun.,* 2012, **48**, 7019-7021; (b) Q. Song, F. Wang, J. Y. Cai, Y. Wang, J. Zhang, W. Q. Yu and J. Xu, *Energy Environ. Sci*., 2013, **6**, 994-1007; (c) R. Ma, W. Hao, X. Ma, Y. Tian and Y. Li, *Angew. Chem. Int. Ed*., 2014, **53**, 1-7; (d) A. L. Jongerius, P. C. A. Bruijnincx and B. M. Weckhuysen, *Green Chem*. 2013, **15**, 3049-3056.
3. (a) A. Corma, S. Iborra and A. Velty, *Chem. Rev*., 2007, **107**, 2411-2502. (b) J. Zakzeski, P. C. A. Bruijnincx, A. L. Jongerius and B. M. Weckhuysen, *Chem. Rev.,* 2010, **110**, 3552-3599; (b) M. Stocker, *Angew. Chem. Int. Ed*., 2008, **47**, 9200-9211; (c) M. Saidi, F. Samimi, D. Karimipourfard, T. Nimanwudipong, B. C. Gates and M. R. Rahimpour, *Energy Environ*. Sci., 2014, **7**, 103-129; (d) T. P. Vispute, H. Zhang, A. Sanna, R. Xiao and G. W. Huber, *Science,* 2010**, 330**, 1222-1227.
4. Y. R. Luo, In Comprehensive Handbook of Chemical Bond Energies; CRC Press: Boca Raton, FL, 2007.
5. (a) A. G. Sergeev and J. F. Hartwig, *Science.,* 2011**, 332**, 439-443; (b) J. M. Nichols, L. M. Bishop, R. G. Bergman and J. A. Ellman, *J. Am. Chem. Soc.,* 2010, **132**, 12554-12555; (c) S. Son and F. D. Toste, *Angew. Chem. Int. Ed*., 2010, **49**, 3791-3794.
6. Y. L. Ren, M.J. Yan, J. J. Wang, Z. C. Zhang and K. S. Yao, *Angew. Chem. Int. Ed.*, 2013, **52**, 12674-12678.
7. (a) J. Zhang, J. Teo, X. Chen, H. Asakura, T. Tanaka, K. Teramura and N. Yan, *ACS Catal*., 2014, **4**, 1574-1583; (b) J. Zhang, H. Asakura, J. Rijn, J. Yang, P. Duchesne, B. Zhang, X. Chen, P. Zhang, M. Saeys and N. Yan, *Green Chem*., 2014, **16**, 2432-2437.
8. (a) A. G. Sergeev, J. D. Webb and J. F. Hartwig, *J. Am. Chem. Soc*., 2012, **134**, 20226-20229; (b) J. He, C. Zhao and J. A. Lercher, *J. Am. Chem. Soc*., 2012, **134**, 20768-20775; (c) J. He, L. Lu, C. Zhao, D. Mei and J. A. Lercher, *J.Catal*., 2014, **311**, 41-51; (d) J. He, C. Zhao, D. Mei and J. A. Lercher, *J.Catal*., 2014, **309**, 280-290.
9. (a) C. Zhao and J. A. Lercher, *Angew. Chem. Int. Ed*., 2012, **51**, 5935-5940; (b) C. Zhao and J. A. Lercher, *ChemCatChem,* 2012, **4**, 64-68; (c) C. Zhao, Y. Kou, A. A. Lemonidou, X. Li and J. A. Lercher, *Angew. Chem. Int. Ed*., 2009, **121**, 4047-4050; (d) C. Zhao, Y. Kou, A. A. Lemonidou, X. Li and J. A. Lercher, *Chem. Commun.,* 2009, **46**, 412-414; (e) W. Zhang, J. Chen, R. Liu, S. Wang, L. Chen and K. Li, *ACS Catal*., 2014, **2**, 683-691; (f) H. Xu, K. Wang, H. Zhang, L. Hao, J. Xu and Z. Liu, *Catal. Sci. Technol*., 2014, **4**, 2658-2663; (g) J. G. Dickinson and P. E. Savage, *ACS Catal*., 2014, **4**, 2605-2615.
10. X. Wang and R. Rinaldi, *Angew. Chem. Int. Ed*., 2013, **52**, 11499-11503.
11. D. J. Rensel, S. Rouvimov, M. E. Gin and J. C. Hicks, *J. Catal*., 2013**, 305**, 256-263.
12. (a) T. Prasomsri, T. Shetty, M. Murugappan and Y. Roman-Leshkov, *Energy Environ. Sci*., 2014**, 7**, 2660-2669; (b) W. Lee, Z. Wang, R. Wu and A. Bhan, *J. Catal*., 2014**, 319**, 44-53.
13. (a) E. P. Maris and R. J. Davis, *J. Catal*., 2007, **249**, 328-337; (b) T. Miyazawa, S. Koso, K. Kunimori and K. Tomishige, *Appl. Catal. A.,* 2007, **318**, 244-251; (c) D. G. Lahr and B. H. Shanks, *J. Catal.,* 2005, **232**, 386; (d) J. Sun and H. Liu, *Green Chem*., 2011**, 13**, 135-142.
14. (a) C. Luo, S. Wang and H. Liu, *Angew. Chem. Int. Ed*., 2007, **46**, 7636-7639; (b) A. Fukuoka and P. L. Dhepe, *Angew. Chem. Int. Ed*., 2006, **45**, 5161-5163; (c) J. Geboers, S. Van de Vyver, K. Carpentier, K. de Blochouse, P. Jacobs and B. F. Sels, *Chem. Commun*., 2010, **46**, 3577-3579; (d) H. Kobayashi, T. Komanoya, K. Hara and A. Fukuoka, *ChemSusChem,* 2010, **3**, 440-443; (e) B. Op de Beeck, J. Geboers, S. Van de Vyver, J. Van Lishout, J. Snelders, W.J. Huijgen, C.M. Courtin, P.A. Jacobs and B.F. Sels, *ChemSusChem,* 2013**, 6***,* 199-208.
15. G. Jerkiewicz, *Electrocatal*., 2010, **1**, 179-199.
16. (a) E. Wilhelm, R. Battino and R. J. Wilcock, *Chem. Rev*., 1977, **77**, 219-262; (b) V. I. Baranenko and V.S. Kirov, *Atomic Energy,* 1989, **66**, 30-34.
17. P. Feulner and D. Menzel, *Surf. Sci*., 1985, **154**, 465-488.
18. J. He, C. Zhao and J. A. Lercher, *J. Catal*., 2014, **309**, 362-375.

ARTICLE

Table of Content: